Immersed boundary method combined with a high order compact scheme on half-staggered meshes

M Księżyk , A Tyliszczak
Czestochowa University of Technology, Institute of Thermal Machinery, Al. AK 21, 42-200 Częstochowa, Poland

E-mail: ksiezykm@imc.pcz.czest.pl

Abstract. This paper presents the results of computations of incompressible flows performed with a high-order compact scheme and the immersed boundary method. The solution algorithm is based on the projection method implemented using the half-staggered grid arrangement in which the velocity components are stored in the same locations while the pressure nodes are shifted half a cell size. The time discretization is performed using the predictor-corrector method in which the forcing terms used in the immersed boundary method acts in both steps. The solution algorithm is verified based on 2D flow problems (flow in a lid-driven skewed cavity, flow over a backward facing step) and turns out to be very accurate on computational meshes comparable with ones used in the classical approaches, i.e. not based on the immersed boundary method.

1. Introduction

Undoubtedly, from the point of view of a solution accuracy none of the discretization method may compete with the spectral and pseudo-spectral methods which are regarded as the most accurate [1]. The weak point of these approaches is that they can be applied in rather simple computational domains and with the nodes distribution and boundary conditions enforced by the type of the method. For instance, the spectral method based on the Fourier series is suited for periodic problems with the uniform mesh points distribution. On the other hand the pseudospectral method based on the Chebyshev polynomials is used mainly in cases which require good resolutions near boundaries, e.g. the wall bounded flows. In this view the high-order compact difference methods [2] seem to be very attractive giving much more possibilities regarding non-uniformity of the computational meshes, selection of the boundary conditions or shapes of computational domains. Although the compact methods cannot compare with flexibility of the finite volume or finite element based methods, they are successfully applied on non-uniform meshes and in irregular domains [3,4,5]. However, this is not a trivial task and often requires domain division, normalisation, co-ordinate transformations, etc. Possibly the easiest solution allowing to use the compact methods in complicated domains is to combine them with the so-called Immersed Boundary (IB) method. Application of this approach seems to be relatively easy and very efficient [6]. The Navier-Stokes equations are solved on Cartesian regular grids with arbitrary boundaries or arbitrary objects embedded directly on the grid points. The influence of such objects on the flow field is enforced by body force terms added to the Navier-Stokes equations [6,7]. The present work focuses on combination of high-order compact method with IB approach for incompressible flows within a framework of the projection method.

It is known that the high-order methods are prone to instabilities near discontinuities or sharp gradients. In the case of IB method such a behaviour could be expected in the vicinity of walls introduced into the flow domain. This paper shows that these problems are very narrowed and practically do not influence the

results. The solution algorithm is validated in enclosed and partially open geometries based on two classical test cases, a flow in a lid-driven skewed cavity and a flow over a backward facing step.
The paper is organised as follow: the governing equations and the solution algorithm are presented in the next section together with details of IB approach. Section 3 presents the results of simulations which are followed by conclusions and future outlook.

2. Mathematical model and numerical algorithm

Fluid flow of an incompressible fluid is governed by the continuity equation and Navier-Stoqes equations given as:

$$\frac{\partial u_i}{\partial x_i} = 0 \tag{1}$$

$$\frac{\partial u_i}{\partial t} + u_j \frac{\partial u_i}{\partial x_j} = -\frac{1}{\rho}\frac{\partial p}{\partial x_i} + \nu \frac{\partial^2 u_i}{\partial x_j^2} + f_{IB} \tag{2}$$

where u_i are velocity components, ρ is density, p - pressure, ν - kinematic viscosity and f_{IB} denotes a source term which will be used to force zero values of velocity at the domain boundaries. We consider flow problems with constant fluid properties, i.e., constant density and viscosity.

2.1 Description of the flow solver

The set of equations (1-2) is solved using the numerical code (SAILOR) which is an academic high-order flow solver based on the low Mach number approximation [8,9]. This code may be used for solving a wide range of flows under various conditions, varying from isothermal and constant density to situations with considerable density and temperature variations. The SAILOR code was used previously in various studies including laminar/turbulent transition in near-wall flows [10] free jet flows [11,12], multi-phase flows [13] and flames [14,15]. The solution algorithm used in the SAILOR code for the case constant density flows is presented in the next subsection. The spatial discretization is based on 6th order compact differencing developed for half-staggered meshes [16]. 'Figure 1' shows locations of the velocity and pressure nodes. Unlike in the fully staggered approach the velocity nodes are common for the velocity components whereas the pressure nodes are moved half a grid size from the velocity nodes. This is computationally efficient as there is only a small amount of interpolation between the nodes. As shown in [16] the staggering of the pressure nodes is sufficient to ensure a strong velocity-pressure coupling which eliminates the well known pressure oscillations occurring on collocated meshes.
The solution algorithm in the SAILOR code is based on the projection method in which the pressure is computed from the Poisson equation. The time advancement of equation (2) is performed with a predictor-corrector method with help of the 2nd order Adams-Bashforth and Adams-Moulton methods.

The predictor step is given as:

- the Navier-Stokes equations are solved as:

$$\frac{u_i^* - u_i^n}{\Delta t} = \left[\frac{3}{2}Res(u^n) - \frac{1}{2}Res(u^{n-1})\right] - \frac{1}{\rho}\frac{\partial p^n}{\partial x_i} + f_{IB} \tag{3}$$

  where $Res(u^n)$ represents the convection and diffusion terms. The upper scripts denote the time level t and t=t-Δt where Δt is the time step. The pressure gradient is computed based on the previous time step. Evaluation of the source term is discussed later in Sec. 2.2.
- in general, the velocity field u^* obtained from equation (3) is not divergence free and need to be corrected; the projection method assumes that the velocity is corrected by pressure gradient as:

$$u_i^{**} = u_i^* - \Delta t \frac{1}{\rho}\frac{\partial p'}{\partial x_i} \tag{4}$$

- requirement $DIV(u^{**})=0$ leads to the Poisson equation for the pressure given as:

$$\frac{\partial}{\partial x_i}\left(\frac{\partial p'}{\partial x_i}\right) = \frac{\rho}{\Delta t}\frac{\partial u_i^*}{\partial x_i} \tag{5}$$

where p' is the pressure correction. Solution of equation (5) allows to correct the velocity according to equation (4).

The corrector step is given as:

- the Navier-Stokes equations in the corrector step are solved with semi-implicit method with the velocity at the time step t=t+Δt assumed equal to u^{**}; hence, the corrector step starts by advancing in time the equation:

$$\frac{u_i^* - u_i^n}{\Delta t} = \frac{1}{2}[Res(u^{**}) + Res(u^n)] - \frac{1}{\rho}\frac{\partial p^n}{\partial x_i} + f_{IB} \tag{6}$$

- similarly as in the predictor step the velocity must be corrected using:

$$u_i^{n+1} = u_i^* - \Delta t \frac{1}{\rho}\frac{\partial p'}{\partial x_i} \tag{7}$$

where the pressure corrections is obtained from the Poisson equation resulting from substitution of equation (6) into $DIV(u^{n+1})=0$. The resulting Poisson equation has the same form as equation (5). Solving it for the pressure correction p' allows to correct the velocity using equation (7), and to update the pressure as $p^{n+1}=p^n+p'$.

2.2 Immersed Boundary (IB) method

The high-order discretisation method applied in the SAILOR code limits its use to the cases with rather simple geometries such as straight or smoothly diverging ducts and channels with smooth bumps. Application of IB method aims to extend applicability of the SAILOR code to the flow problems with almost arbitrary non-rectangular domains and cases with flows around objects embedded inside the computational domains.

The algorithm presented in the previous section did not include the forcing term present in equation (2). In general there are two options of the IB method called feedback forcing method [17] and direct forcing method [6]. They differ in evaluation of the forcing term. In this work the latter approach is implemented which seems to be simpler and more efficient. Interested reader is referred to [18] where all details and variants of IB methods may be found. Here we limit ourselves to explain how the term f_{IB} is computed. In the predictor step it is defined as:

$$f_{IB} = \frac{u_{WALL}^* - u_i^n}{\Delta t} - \left[\frac{3}{2}Res(u^n) - \frac{1}{2}Res(u^{n-1})\right] - \frac{1}{\rho}\frac{\partial p^n}{\partial x_i} \tag{8}$$

where the symbol u_{WALL} stands for the velocity at the wall which is a part of the computational domain as shown in 'figure 1' by black sold line. The velocity on that boundary is known and this allows to estimate the values of velocity in its closest vicinity, i.e., in the computational nodes shown in 'figure 1' by black squares. In the present approach the velocity in these nodes is obtained from the 2nd order linear interpolation based on the velocity values from the second node line from the boundary (shown by high arrow in 'figure 1') and the desired boundary values. As will be shown later, although the 2nd order interpolation locally reduces the formal approximation order it does not influence significantly on the results far from the immersed boundaries. Inside the immersed body, i.e., in the nodes with

crosses the velocity is forced to a given velocity of the body. In the test cases presented in the next section we assume stationary bodies, however it should be clear that the IB method allows to simulate moving objects as well. We note that in the corrector step the source term is evaluated similarly but based on equation (6).

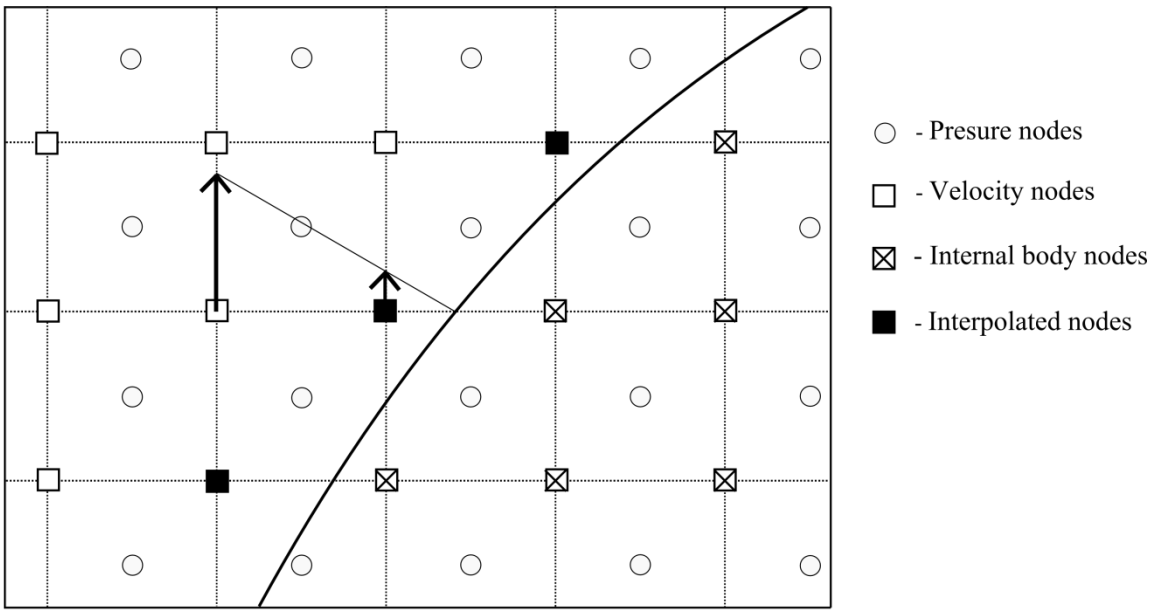

Figure 1. Linear velocity interpolation method.

3. Results

Correctness of the high-order code combined with IB method is verified based on 2D flow problems commonly used in literature as exemplary test cases: a flow inside a lid-driven skewed cavity [19] and a flow over a backward-facing step [20]. The literature data [19, 20] used as the reference solutions were obtained using the classical approach, i.e., with the computational meshes fitted with domain boundaries. Although, the following validation has been performed only for 2D steady state cases it clearly confirms very large potential of IB method.

3.1 Flow inside a skewed cavity

The flow domain for this test case is shown in 'figure 2'. The angle at which the cavity leans is equal α=135°. The dimensions of the cavity were normalized using the length of the upper wall (L) whereas the velocity field was normalized by the horizontal velocity (U) of that wall. The computations were performed for Reynolds number $Re=UL/\nu=1000$. The computational domain covered the region of the cavity and also the region outside of the cavity, i.e., $x \in (0, 1.707)$ and $y \in (0, 0.707)$. Two mesh densities were used with 128x309 nodes and 256x618 nodes (the first numbers refer to the vertical direction). The number of nodes inside the cavity in the horizontal direction was equal to 181 for the coarse mesh and 362 for the refined mesh. In both the cases the solutions were smooth and there was no signs of oscillations or pronounced discontinuities near the boundaries. In the velocity or pressure field only very small wrinkles were observed. The velocity components in the nodes outside the cavity were of the order of 10^{-2} and maximum values occurred near the upper corners. As an example the 'figure 3' shows the velocity modulus. It is seen that outside the boundaries the velocity is not exactly zero. In these nodes the velocity is artificially set to zero before the next time step begins. 'Figure 4 and 5' show the comparisons of the horizontal and vertical velocity profiles along the lines A-B and C-D defined in 'figure 2'. The reference solution [19] presented in 'figures 4 and 5' was obtained with a very dense mesh with 513x513 nodes inside the cavity. As may be seen the present results obtained on the coarse mesh are far from the reference data, although the general flow behaviour is predicted relatively well. Increasing the number of nodes significantly improves the solution accuracy.

It is seen that on the denser mesh both velocity components are predicted very accurately and the present results almost perfectly match the literature data. Worth noting is that on the denser mesh the number of nodes inside the cavity is still smaller than in the computations performed in [19]. Excellent accuracy of the present solution is attributed to the high-order discretization method which turns out to compensate errors resulting from IB approach on the boundaries.

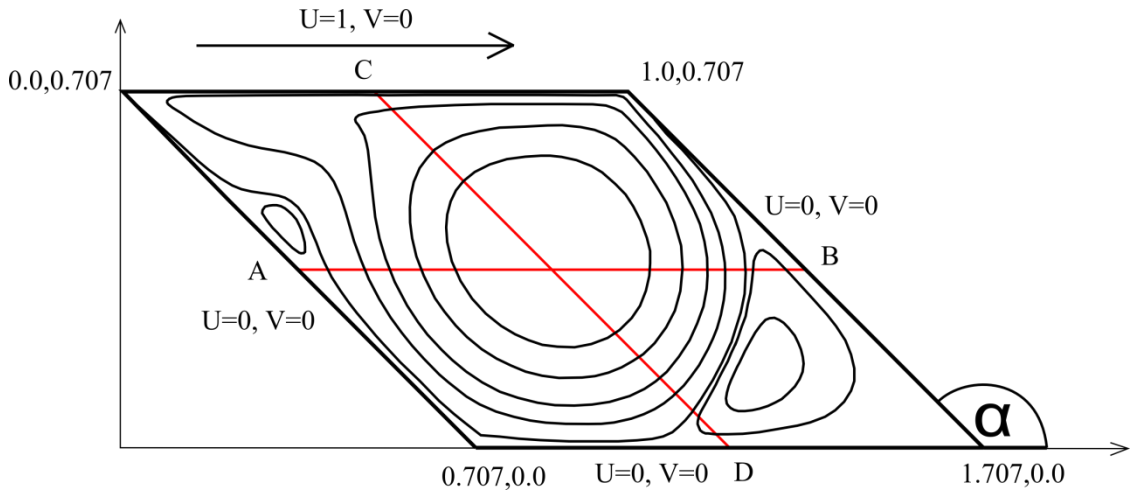

Figure 2. Schematic view with streamline contours of the skewed cavity flow.

3.2 Flow over a backward-facing step

The computational domain for this test case is shown in 'figure 6'. The length of the domain is 40*h* where *h* is the step height. The length of the step is 2*h* and in this region the velocity is forced to zero. The computations were performed for *Re=Uh/v=800* where *U* is the mean velocity at the inlet where the parabolic velocity profiles was prescribed with the maximum value equal to 1.5. Two computational meshes were used with 49x980 nodes and 75x1024 nodes. Unlike as in the previous example the results on these meshes were very similar, particularly further downstream the step. 'Figure 6' presents the streamlines showing the locations of recirculation zones (RZ) at the upper and the lower wall of the channel. The length of the lower RZ is equal to 12h while the upper RZ extends over 9.5*h*-20.5*h*. A reference solution [20] was obtained using the mesh with 101x1000 nodes. In this case the length of the lower RZ was equal to 11.834h and the upper RZ was between 9.476-20.553 which is very close to the values obtained presently.

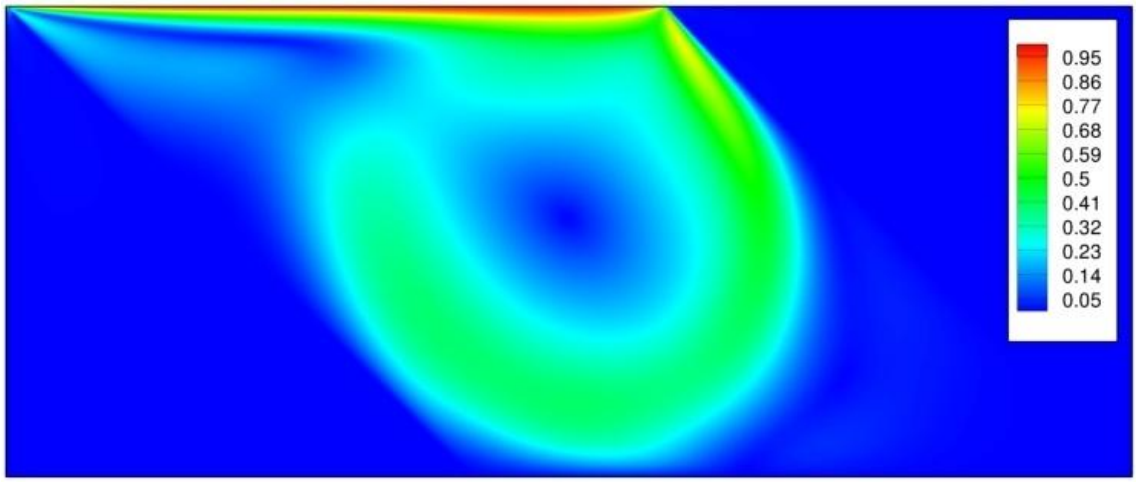

Figure 3. Modulus of the velocity field inside the skewed cavity flow.

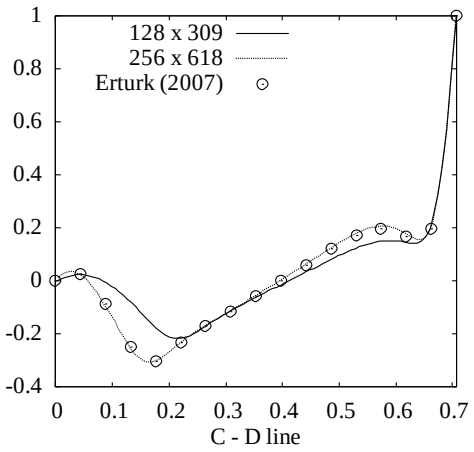

Figure 4. Horizontal velocity component along C-D line.

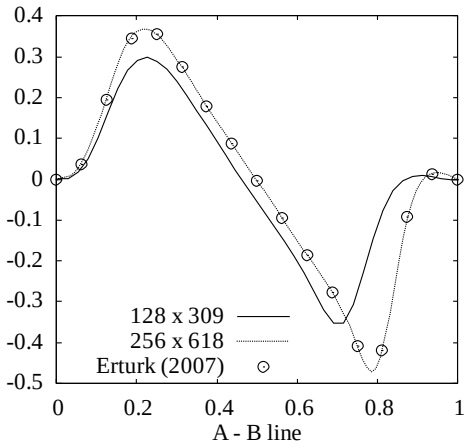

Figure 5. Vertical velocity component along A-B line.

Correctness of the results is further confirmed in comparisons of the horizontal velocity profiles extracted from the solutions at x=6h, x=14h and x=30h. These solutions are shown in 'figures 7, 8 and 9'. It is seen that the results obtained on both meshes are very close each other and also in very good agreement with the exemplary solutions. As in the previous example we connect this behaviour to high-order discretization method.

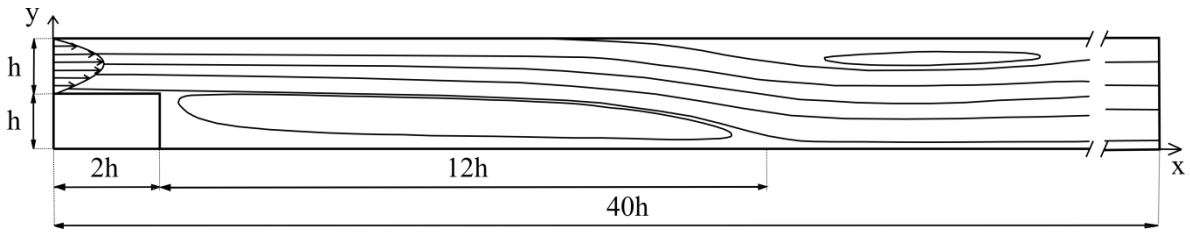

Figure 6. Schematic view with streamline contours of backward facing step.

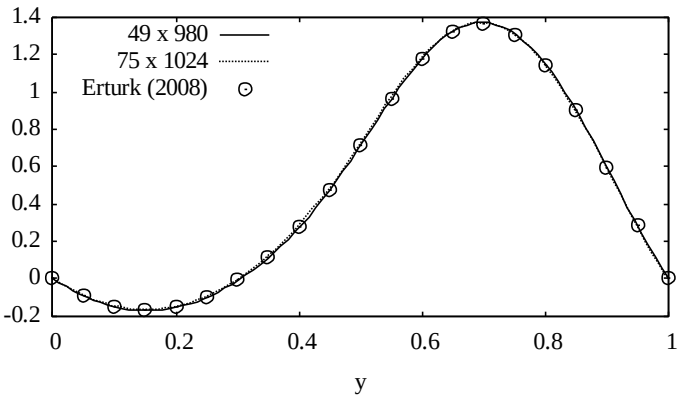

Figure 7. Horizontal velocity profile at x=6h.

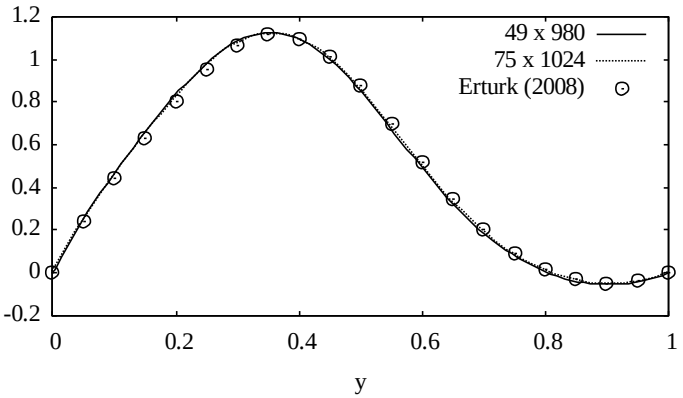

Figure 8. Horizontal velocity profile at x=14h.

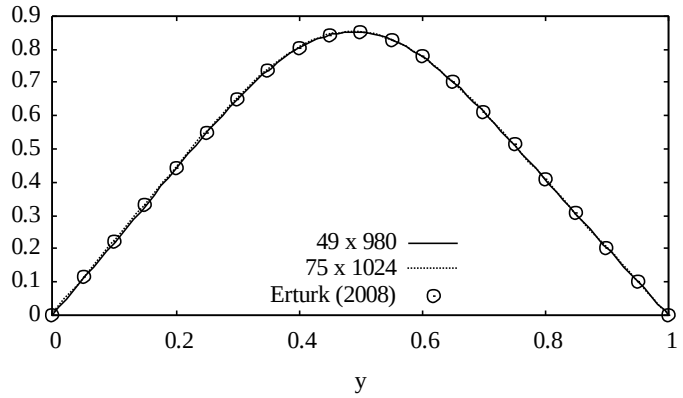

Figure 9. Horizontal velocity profile at x=30h.

4. Conclusions

The paper presented the validation of combination of the high-order compact discretisation with the immersed boundary method. The obtained results were smooth and did not show any signs of instability which could be expected due to the presence of the forcing term used in immersed boundary approach. The obtained solutions were in very good with literature data both for the case of the flow inside the skewed cavity as well as for the flow over the sharp step. Future works will concentrate on validation of the results for unsteady problems and 3D cases.

Acknowledgment*:* The investigation was supported by Polish National Science Centre under Grant no. DEC-2012/07/B/ST8/03791.
This research was also supported in part by PL-Grid Infrastructure (Poland).

5. References

[1] Canuto C, Hussaini M Y, Quarteroni A and Zang T A, 1988 Spectral methods in fluid dynamics *Springer-Verlag*
[2] Lele S K, 1992 Compact Finite Schemes with Spektral-like Resolution *J. Comp. Phys.* **103** 16-42
[3] Sengupta T K, Dipankar A and Kameswara Rao A, 2007 A new compact scheme for parallel computing using domain decomposition *J. Comp. Phys.* **220** 654-677
[4] Pandit S K, Kalita J C and Dalal D C, 2007 A transient higher order compact scheme for incompressible viscous flows on geometries beyond rectangular *J. Comp. Phys.* **225** 1100-1124

[5] Kuban L, Laval J-P, Elsner W, Tyliszczak A, Marquillie M 2012 LES modelling of converging-diverging turbulent channel flow *J. Turb.* **13** 1-19
[6] Mohd-Yosuf J 1997 Combined immersed-boundary/B-spline methods for simulations of flow in complex geometries *Ann. Res. B. Cent. Turb. Res.*
[7] Peskin C S, 1972 Flow patterns around heart valves: a numerical method *J. Comp. Phys.* **10** 252-271
[8] Heuveline V 2003 On higher-order mixed FEM for low Mach number: application to a natural convection benchmark problem *Int. J. Numer. Meth. Fl.* **41** 1339-1356
[9] Knikker R 2011 A comparative study of high-order variable-property segregated algorithms for unsteady low Mach number flows *Int. J. Numer. Meth. Fl.* **66** 403-427
[10] Tyliszczak A, Boguslawski A, Drobniak S 2008 Quality of LES predictions of isothermal and hot round jet *Quality and Reliability of Large Eddy Simulations, Eroftac Series. Turb.* **12** 259-270
[11] Bogusławski A, Tyliszczak A, Drobniak S, Asendrych D 2013 Self-sustained oscillations in a homogeneous-density round jet *J. Turb.* **14** 25-52
[12] Aniszewski W, Bogusławski A, Marek M, Tyliszczak 2012 A New Approach to Sub-grid Surface Tension for LES of Two-phase Flows *J. Comput. Phys.* **231** 7368-7397
[13] Tyliszczak A 2013 Assessment of implementation variants of conditional scalar dissipation rate in LES-CMC simulation of auto-ignition of hydrogen jet *Arch. Mech.* **65** 97-129
[14] Tyliszczak A 2013 LES-CMC and LES-Flamelet simulation of non-premixed methane flame (Sandia F) *J. Theor. Appl. Mech.* **51** 859-871
[15] Laizet S, Lamballais E 2009 High-order compact schemes for incompressible flows: A simple and efficient method with quasi-spectral accuracy *J. Comput. Phys.* **228** 5989-6015
[16] Tyliszczak A 2013 A high-order compact difference algorithm for half-staggered grids for laminar and turbulent incompressible flows *Submitted to J. Comput. Phys.*
[17] Verzicco R, Iaccarino G 2003 Immersed boundary technique for turbulent flow simulations *Appl. Mech. Rev.* **56** 331-347
[18] Mittal R, Iaccarino G 2005 Immersed Boundary Methods *Annu. Rev. Fluid Mech.* **37** 239-261
[19] Erturk E, Dursun B 2007 Numerical solutions of 2-D steady incompressible flow in a driven skewed cavity *J. App. Math. and Mech.* **87** 377-392
[20] Erturk E 2008 Numerical solutions of 2-D steady incompressible flow over a backward-facing step, Part I: High Reynolds number solutions *Comp. Fluids* **37** 633-655